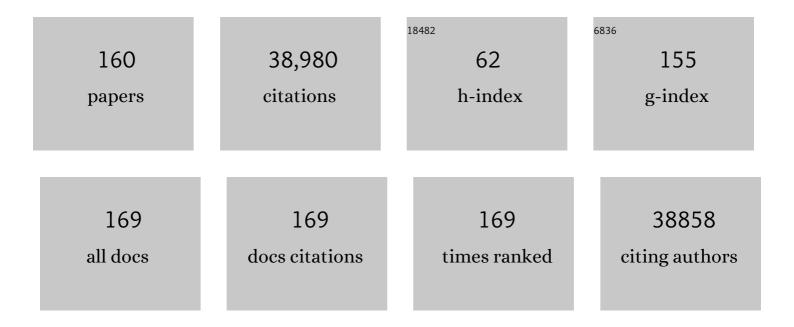
Valeria Nicolosi

List of Publications by Year in descending order

Source: https://exaly.com/author-pdf/6050419/publications.pdf Version: 2024-02-01



#	Article	IF	CITATIONS
1	Two-Dimensional Nanosheets Produced by Liquid Exfoliation of Layered Materials. Science, 2011, 331, 568-571.	12.6	6,190
2	High-yield production of graphene by liquid-phase exfoliation of graphite. Nature Nanotechnology, 2008, 3, 563-568.	31.5	5,431
3	Liquid Exfoliation of Layered Materials. Science, 2013, 340, .	12.6	3,109
4	Science and technology roadmap for graphene, related two-dimensional crystals, and hybrid systems. Nanoscale, 2015, 7, 4598-4810.	5.6	2,452
5	Liquid Phase Production of Graphene by Exfoliation of Graphite in Surfactant/Water Solutions. Journal of the American Chemical Society, 2009, 131, 3611-3620.	13.7	2,038
6	Scalable production of large quantities of defect-free few-layer graphene by shear exfoliation in liquids. Nature Materials, 2014, 13, 624-630.	27.5	1,958
7	Atom-by-atom structural and chemical analysis by annular dark-field electron microscopy. Nature, 2010, 464, 571-574.	27.8	1,138
8	Oxidation Stability of Colloidal Two-Dimensional Titanium Carbides (MXenes). Chemistry of Materials, 2017, 29, 4848-4856.	6.7	1,120
9	Large cale Exfoliation of Inorganic Layered Compounds in Aqueous Surfactant Solutions. Advanced Materials, 2011, 23, 3944-3948.	21.0	1,012
10	Liquid exfoliation of solvent-stabilized few-layer black phosphorus for applications beyond electronics. Nature Communications, 2015, 6, 8563.	12.8	921
11	Transparent, Flexible, and Conductive 2D Titanium Carbide (MXene) Films with High Volumetric Capacitance. Advanced Materials, 2017, 29, 1702678.	21.0	756
12	Additive-free MXene inks and direct printing of micro-supercapacitors. Nature Communications, 2019, 10, 1795.	12.8	649
13	Transition metal nitrides for electrochemical energy applications. Chemical Society Reviews, 2021, 50, 1354-1390.	38.1	580
14	Edge and confinement effects allow in situ measurement of size and thickness of liquid-exfoliated nanosheets. Nature Communications, 2014, 5, 4576.	12.8	432
15	Stamping of Flexible, Coplanar Microâ€Supercapacitors Using MXene Inks. Advanced Functional Materials, 2018, 28, 1705506.	14.9	427
16	A Commercial Conducting Polymer as Both Binder and Conductive Additive for Silicon Nanoparticle-Based Lithium-Ion Battery Negative Electrodes. ACS Nano, 2016, 10, 3702-3713.	14.6	394
17	All-printed thin-film transistors from networks of liquid-exfoliated nanosheets. Science, 2017, 356, 69-73.	12.6	391
18	A stable, wideband tunable, near transform-limited, graphene-mode-locked, ultrafast laser. Nano Research, 2010, 3, 653-660.	10.4	351

#	Article	IF	CITATIONS
19	Quantitative Evaluation of Surfactant-stabilized Single-walled Carbon Nanotubes: Dispersion Quality and Its Correlation with Zeta Potential. Journal of Physical Chemistry C, 2008, 112, 10692-10699.	3.1	343
20	Towards Solutions of Singleâ€Walled Carbon Nanotubes in Common Solvents. Advanced Materials, 2008, 20, 1876-1881.	21.0	333
21	Debundling of Single-Walled Nanotubes by Dilution:Â Observation of Large Populations of Individual Nanotubes in Amide Solvent Dispersions. Journal of Physical Chemistry B, 2006, 110, 15708-15718.	2.6	330
22	Graphene and MXene-based transparent conductive electrodes and supercapacitors. Energy Storage Materials, 2019, 16, 102-125.	18.0	313
23	Layered Orthorhombic Nb ₂ O ₅ @Nb ₄ C ₃ T <i>_x</i> and TiO ₂ @Ti ₃ C ₂ T <i>_x</i> Hierarchical Composites for High Performance Liâ€ion Batteries. Advanced Functional Materials. 2016. 26. 4143-4151.	14.9	309
24	Basal-Plane Functionalization of Chemically Exfoliated Molybdenum Disulfide by Diazonium Salts. ACS Nano, 2015, 9, 6018-6030.	14.6	293
25	High areal capacity battery electrodes enabled by segregated nanotube networks. Nature Energy, 2019, 4, 560-567.	39.5	281
26	3D MXene Architectures for Efficient Energy Storage and Conversion. Advanced Functional Materials, 2020, 30, 2000842.	14.9	276
27	Production of Molybdenum Trioxide Nanosheets by Liquid Exfoliation and Their Application in High-Performance Supercapacitors. Chemistry of Materials, 2014, 26, 1751-1763.	6.7	266
28	High capacity silicon anodes enabled by MXene viscous aqueous ink. Nature Communications, 2019, 10, 849.	12.8	253
29	Highly flexible and transparent solid-state supercapacitors based on RuO2/PEDOT:PSS conductive ultrathin films. Nano Energy, 2016, 28, 495-505.	16.0	247
30	In Situ Formed Protective Barrier Enabled by Sulfur@Titanium Carbide (MXene) Ink for Achieving High apacity, Long Lifetime Li‧ Batteries. Advanced Science, 2018, 5, 1800502.	11.2	210
31	Nano-particle mediated M2 macrophage polarization enhances bone formation and MSC osteogenesis in an IL-10 dependent manner. Biomaterials, 2020, 239, 119833.	11.4	207
32	Preparation of Gallium Sulfide Nanosheets by Liquid Exfoliation and Their Application As Hydrogen Evolution Catalysts. Chemistry of Materials, 2015, 27, 3483-3493.	6.7	195
33	Brownian Motion of Graphene. ACS Nano, 2010, 4, 7515-7523.	14.6	194
34	Multifunctional Ti ₃ C ₂ T _{<i>x</i>} MXene Composite Hydrogels with Strain Sensitivity toward Absorption-Dominated Electromagnetic-Interference Shielding. ACS Nano, 2021, 15, 1465-1474.	14.6	194
35	Quantifying the factors limiting rateÂperformance in battery electrodes. Nature Communications, 2019, 10, 1933.	12.8	185
36	An investigation of nanostructured thin film α-MoO3 based supercapacitor electrodes in an aqueous electrolyte. Electrochimica Acta, 2013, 91, 253-260.	5.2	177

#	Article	IF	CITATIONS
37	Gentle STEM: ADF imaging and EELS at low primary energies. Ultramicroscopy, 2010, 110, 935-945.	1.9	174
38	Collagen scaffolds functionalised with copper-eluting bioactive glass reduce infection and enhance osteogenesis and angiogenesis both in vitro and in vivo. Biomaterials, 2019, 197, 405-416.	11.4	146
39	Fabrication and Characterization of Silver/Polyaniline Composite Nanowires in Porous Anodic Alumina. Chemistry of Materials, 2007, 19, 4252-4258.	6.7	123
40	Liquid exfoliation of interlayer spacing-tunable 2D vanadium oxide nanosheets: High capacity and rate handling Li-ion battery cathodes. Nano Energy, 2017, 39, 151-161.	16.0	123
41	Ionic liquid pre-intercalated MXene films for ionogel-based flexible micro-supercapacitors with high volumetric energy density. Journal of Materials Chemistry A, 2019, 7, 9478-9485.	10.3	120
42	Ordered DNA Wrapping Switches on Luminescence in Single-Walled Nanotube Dispersions. Journal of the American Chemical Society, 2008, 130, 12734-12744.	13.7	119
43	The relationship between network morphology and conductivity in nanotube films. Journal of Applied Physics, 2008, 104, .	2.5	119
44	All-pseudocapacitive asymmetric MXene-carbon-conducting polymer supercapacitors. Nano Energy, 2020, 75, 104971.	16.0	119
45	Enhanced thermoelectric performance of Bi–Sb–Te/Sb ₂ O ₃ nanocomposites by energy filtering effect. Journal of Materials Chemistry A, 2018, 6, 21341-21349.	10.3	116
46	Additive Manufacturing of Ti ₃ C ₂ â€MXeneâ€Functionalized Conductive Polymer Hydrogels for Electromagneticâ€Interference Shielding. Advanced Materials, 2022, 34, e2106253.	21.0	115
47	Advanced materials of printed wearables for physiological parameter monitoring. Materials Today, 2020, 32, 147-177.	14.2	110
48	MXene materials based printed flexible devices for healthcare, biomedical and energy storage applications. Materials Today, 2021, 43, 99-131.	14.2	107
49	Solubility of Mo6S4.5I4.5Nanowires in Common Solvents:Â A Sedimentation Study. Journal of Physical Chemistry B, 2005, 109, 7124-7133.	2.6	105
50	Spontaneous Debundling of Single-Walled Carbon Nanotubes in DNA-Based Dispersions. Journal of Physical Chemistry C, 2007, 111, 66-74.	3.1	93
51	Effect of Percolation on the Capacitance of Supercapacitor Electrodes Prepared from Composites of Manganese Dioxide Nanoplatelets and Carbon Nanotubes. ACS Nano, 2014, 8, 9567-9579.	14.6	89
52	Nitrogen-doped reduced graphene oxide electrodes for electrochemical supercapacitors. Physical Chemistry Chemical Physics, 2014, 16, 2280.	2.8	87
53	The rationale and emergence of electroconductive biomaterial scaffolds in cardiac tissue engineering. APL Bioengineering, 2019, 3, 041501.	6.2	84
54	Oxide-mediated recovery of field-effect mobility in plasma-treated MoS ₂ . Science Advances, 2018, 4, eaao5031.	10.3	82

#	Article	IF	CITATIONS
55	Laser synthesis of Au/Ag colloidal nano-alloys: Optical properties, structure and composition. Applied Surface Science, 2007, 254, 1007-1011.	6.1	76
56	Large Populations of Individual Nanotubes in Surfactant-Based Dispersions without the Need for Ultracentrifugation. Journal of Physical Chemistry C, 2008, 112, 972-977.	3.1	75
57	Covalently Functionalized Hexagonal Boron Nitride Nanosheets by Nitrene Addition. Chemistry - A European Journal, 2012, 18, 10808-10812.	3.3	75
58	Quantifying the Effect of Electronic Conductivity on the Rate Performance of Nanocomposite Battery Electrodes. ACS Applied Energy Materials, 2020, 3, 2966-2974.	5.1	75
59	Covalently interconnected transition metal dichalcogenide networks via defect engineering for high-performance electronic devices. Nature Nanotechnology, 2021, 16, 592-598.	31.5	74
60	Production of Ni(OH) ₂ nanosheets by liquid phase exfoliation: from optical properties to electrochemical applications. Journal of Materials Chemistry A, 2016, 4, 11046-11059.	10.3	71
61	Enabling Flexible Heterostructures for Liâ€lon Battery Anodes Based on Nanotube and Liquidâ€Phase Exfoliated 2D Gallium Chalcogenide Nanosheet Colloidal Solutions. Small, 2017, 13, 1701677.	10.0	71
62	Two-dimensional material inks. Nature Reviews Materials, 2022, 7, 717-735.	48.7	71
63	Double-Wall Carbon Nanotubes for Wide-Band, Ultrafast Pulse Generation. ACS Nano, 2014, 8, 4836-4847.	14.6	66
64	Spectroscopic evidence of a core–shell structure in the earlier formation stages of Au–Ag nanoparticles by pulsed laser ablation in water. Chemical Physics Letters, 2008, 457, 386-390.	2.6	60
65	Probing the local nature of excitons and plasmons in few-layer MoS2. Npj 2D Materials and Applications, 2017, 1, .	7.9	58
66	Comparison of carbon nanotubes and nanodisks as percolative fillers in electrically conductive composites. Scripta Materialia, 2008, 58, 69-72.	5.2	56
67	High Quality Dispersions of Functionalized Single Walled Nanotubes at High Concentration. Journal of Physical Chemistry C, 2008, 112, 3519-3524.	3.1	56
68	Low-temperature synthesis and investigation into the formation mechanism of high quality Ni-Fe layered double hydroxides hexagonal platelets. Scientific Reports, 2018, 8, 4179.	3.3	56
69	Solubility of Mo6S4.5I4.5 nanowires. Chemical Physics Letters, 2005, 401, 13-18.	2.6	55
70	Structural transformation of layered double hydroxides: an in situ TEM analysis. Npj 2D Materials and Applications, 2018, 2, .	7.9	53
71	Charge transport mechanisms in inkjet-printed thin-film transistors based on two-dimensional materials. Nature Electronics, 2021, 4, 893-905.	26.0	52
72	Twoâ€₽hoton Absorption in Monolayer MXenes. Advanced Optical Materials, 2020, 8, 1902021.	7.3	50

#	Article	IF	CITATIONS
73	High Quality Dispersions of Hexabenzocoronene in Organic Solvents. Journal of the American Chemical Society, 2012, 134, 12168-12179.	13.7	49
74	Improving stability of organometallic-halide perovskite solar cells using exfoliation two-dimensional molybdenum chalcogenides. Npj 2D Materials and Applications, 2020, 4, .	7.9	49
75	Scaleable ultra-thin and high power density graphene electrochemical capacitor electrodes manufactured by aqueous exfoliation and spray deposition. Carbon, 2013, 52, 337-346.	10.3	47
76	Electronic Properties and Chemical Reactivity of TiS ₂ Nanoflakes. Journal of Physical Chemistry C, 2015, 119, 15707-15715.	3.1	47
77	A 2D graphene-manganese oxide nanosheet hybrid synthesized by a single step liquid-phase co-exfoliation method for supercapacitor applications. Electrochimica Acta, 2015, 174, 696-705.	5.2	47
78	One-Dimensional (1D) Nanostructured Materials for Energy Applications. Materials, 2021, 14, 2609.	2.9	47
79	Exfoliation in ecstasy: liquid crystal formation and concentration-dependent debundling observed for single-wall nanotubes dispersed in the liquid drug γ-butyrolactone. Nanotechnology, 2007, 18, 455705.	2.6	45
80	Production of Quasi-2D Platelets of Nonlayered Iron Pyrite (FeS ₂) by Liquid-Phase Exfoliation for High Performance Battery Electrodes. ACS Nano, 2020, 14, 13418-13432.	14.6	45
81	A study of the charge storage properties of a MoSe2 nanoplatelets/SWCNTs electrode in a Li-ion based electrolyte. Electrochimica Acta, 2016, 192, 1-7.	5.2	44
82	Unusual Stacking Variations in Liquid-Phase Exfoliated Transition Metal Dichalcogenides. ACS Nano, 2014, 8, 3690-3699.	14.6	43
83	Quantifying the Tradeâ€Off between Absolute Capacity and Rate Performance in Battery Electrodes. Advanced Energy Materials, 2019, 9, 1901359.	19.5	43
84	Gas phase controlled deposition of high quality large-area graphene films. Chemical Communications, 2010, 46, 1422.	4.1	42
85	Edge-carboxylated graphene nanoflakes from nitric acid oxidised arc-discharge material. Journal of Materials Chemistry, 2010, 20, 314-319.	6.7	41
86	A safe-by-design approach to the development of gold nanoboxes as carriers for internalization into cancer cells. Biomaterials, 2014, 35, 2543-2557.	11.4	41
87	Rhenium-doped MoS2 films. Applied Physics Letters, 2017, 111, .	3.3	40
88	Liquid Exfoliated SnP ₃ Nanosheets for Very High Areal Capacity Lithiumâ€lon Batteries. Advanced Energy Materials, 2021, 11, 2002364.	19.5	40
89	Orthopaedic implant materials drive M1 macrophage polarization in a spleen tyrosine kinase- and mitogen-activated protein kinase-dependent manner. Acta Biomaterialia, 2018, 65, 426-435.	8.3	39
90	Improving the performance of porous nickel foam for water oxidation using hydrothermally prepared Ni and Fe metal oxides. Sustainable Energy and Fuels, 2017, 1, 207-216.	4.9	38

#	Article	IF	CITATIONS
91	Novel cold spray for fabricating graphene-reinforced metal matrix composites. Materials Letters, 2017, 196, 172-175.	2.6	36
92	Valence band modification of Cr ₂ O ₃ by Ni-doping: creating a high figure of merit p-type TCO. Journal of Materials Chemistry C, 2017, 5, 12610-12618.	5.5	36
93	Dispersion and purification of Mo6S3I6 nanowires in organic solvents. Journal of Applied Physics, 2007, 101, 014317.	2.5	35
94	Liquid phase exfoliation of MoO ₂ nanosheets for lithium ion battery applications. Nanoscale Advances, 2019, 1, 1560-1570.	4.6	35
95	Extra lithium-ion storage capacity enabled by liquid-phase exfoliated indium selenide nanosheets conductive network. Energy and Environmental Science, 2020, 13, 2124-2133.	30.8	35
96	Interfacial Engineered Vanadium Oxide Nanoheterostructures Synchronizing High-Energy and Long-Term Potassium-Ion Storage. ACS Nano, 2022, 16, 1502-1510.	14.6	35
97	Controlled Radiation Damage and Edge Structures in Boron Nitride Membranes. ACS Nano, 2011, 5, 3977-3986.	14.6	33
98	Quantifying the Role of Nanotubes in Nano:Nano Composite Supercapacitor Electrodes. Advanced Energy Materials, 2018, 8, 1702364.	19.5	33
99	Spontaneous Exfoliation of Single-Walled Carbon Nanotubes Dispersed Using a Designed Amphiphilic Peptide. Biomacromolecules, 2008, 9, 598-602.	5.4	32
100	Direct atomic scale determination of magnetic ion partition in a room temperature multiferroic material. Scientific Reports, 2017, 7, 1737.	3.3	32
101	Debundling by dilution: Observation of significant populations of individual MoSI nanowires in high concentration dispersions. Chemical Physics Letters, 2006, 425, 89-93.	2.6	28
102	Manganese oxide nanosheets and a 2D hybrid of graphene–manganese oxide nanosheets synthesized by liquid-phase exfoliation. 2D Materials, 2015, 2, 025005.	4.4	28
103	TiO ₂ -Based Nanomaterials for the Production of Hydrogen and the Development of Lithium-Ion Batteries. Journal of Physical Chemistry B, 2018, 122, 972-983.	2.6	28
104	Pushing up the magnetisation values for iron oxide nanoparticles via zinc doping: X-ray studies on the particle's sub-nano structure of different synthesis routes. Physical Chemistry Chemical Physics, 2016, 18, 25221-25229.	2.8	27
105	Atomic scale dynamics of a solid state chemical reaction directly determined by annular dark-field electron microscopy. Scientific Reports, 2014, 4, 7555.	3.3	26
106	Layered Double Hydroxide as a Potent Non-viral Vector for Nucleic Acid Delivery Using Gene-Activated Scaffolds for Tissue Regeneration Applications. Pharmaceutics, 2020, 12, 1219.	4.5	26
107	Solution processed thin film transistor from liquid phase exfoliated MoS2 flakes. Solid-State Electronics, 2018, 141, 58-64.	1.4	24
108	Oxygen evolution catalysts under proton exchange membrane conditions in a conventional three electrode cell <i>vs.</i> electrolyser device: a comparison study and a 3D-printed electrolyser for academic labs. Journal of Materials Chemistry A, 2021, 9, 9113-9123.	10.3	24

#	Article	IF	CITATIONS
109	An in situ and ex situ TEM study into the oxidation of titanium (IV) sulphide. Npj 2D Materials and Applications, 2017, 1, .	7.9	21
110	Impurity induced non-bulk stacking in chemically exfoliated h-BN nanosheets. Nanoscale, 2013, 5, 2290.	5.6	20
111	An investigation of the energy storage properties of a 2D <i>α</i> -MoO ₃ -SWCNTs composite films. 2D Materials, 2017, 4, 015005.	4.4	20
112	Lithium Titanate/Carbon Nanotubes Composites Processed by Ultrasound Irradiation as Anodes for Lithium Ion Batteries. Scientific Reports, 2017, 7, 7614.	3.3	17
113	Quantifying the Effect of Separator Thickness on Rate Performance in Lithium-Ion Batteries. Journal of the Electrochemical Society, 2022, 169, 030503.	2.9	17
114	High mobility solution processed MoS2 thin film transistors. Solid-State Electronics, 2019, 158, 75-84.	1.4	16
115	Quantifying the Dependence of Battery Rate Performance on Electrode Thickness. ACS Applied Energy Materials, 2020, 3, 10154-10163.	5.1	16
116	Using chronoamperometry to rapidly measure and quantitatively analyse rate-performance in battery electrodes. Journal of Power Sources, 2020, 468, 228220.	7.8	16
117	Nonlinear optical response of Mo6S4.5I4.5 nanowires. Chemical Physics Letters, 2007, 435, 109-113.	2.6	15
118	pH-Responsive Saloplastics Based on Weak Polyelectrolytes: From Molecular Processes to Material Scale Properties. Macromolecules, 2018, 51, 4424-4434.	4.8	15
119	Liquid phase exfoliation of nonlayered non-van der Waals iron trifluoride (FeF3) into 2D-platelets for high-capacity lithium storing cathodes. FlatChem, 2022, 33, 100360.	5.6	15
120	Single-step exfoliation and chemical functionalisation of graphene and hBN nanosheets with nickel phthalocyanine. Journal of Materials Chemistry, 2012, 22, 23246.	6.7	14
121	Silver nanocolloid generation using dynamic Laser Ablation Synthesis in Solution system and drop-casting. Nano Structures Nano Objects, 2022, 29, 100841.	3.5	14
122	A comparison of catabolic pathways induced in primary macrophages by pristine single walled carbon nanotubes and pristine graphene. RSC Advances, 2016, 6, 65299-65310.	3.6	13
123	Percolating Metallic Structures Templated on Laser-Deposited Carbon Nanofoams Derived from Graphene Oxide: Applications in Humidity Sensing. ACS Applied Nano Materials, 2018, 1, 1828-1835.	5.0	12
124	Postsynthetic treatment of nickel–iron layered double hydroxides for the optimum catalysis of the oxygen evolution reaction. Npj 2D Materials and Applications, 2021, 5, .	7.9	12
125	Laser-powder bed fusion of silicon carbide reinforced 316L stainless steel using a sinusoidal laser scanning strategy. Journal of Materials Research and Technology, 2022, 18, 2672-2698.	5.8	12
126	Influence of temperature on morphological and optical properties of MoS2 layers as grown based on solution processed precursor. Thin Solid Films, 2018, 645, 38-44.	1.8	11

#	Article	IF	CITATIONS
127	Solvent engineered synthesis of layered SnO for high-performance anodes. Npj 2D Materials and Applications, 2021, 5, .	7.9	11
128	Extending the Cyclability of Alkaline Zinc–Air Batteries: Synergistic Roles of Li ⁺ and K ⁺ lons in Electrodics. ACS Applied Materials & Interfaces, 2021, 13, 33112-33122.	8.0	11
129	Novel in-situ lamella fabrication technique for in-situ TEM. Ultramicroscopy, 2018, 190, 21-29.	1.9	10
130	Synthesis of centimeter-size free-standing perovskite nanosheets from single-crystal lead bromide for optoelectronic devices. Scientific Reports, 2019, 9, 11738.	3.3	9
131	Selfâ€Assembly of Atomically Thin Chiral Copper Heterostructures Templated by Black Phosphorus. Advanced Functional Materials, 2019, 29, 1903120.	14.9	9
132	Temperature influence on Ti3C2Tx lines printed by aerosol jet printing. Sensors and Actuators A: Physical, 2021, 332, 113185.	4.1	9
133	One-Step Grown Carbonaceous Germanium Nanowires and Their Application as Highly Efficient Lithium-Ion Battery Anodes. ACS Applied Energy Materials, 2022, 5, 1922-1932.	5.1	9
134	EELS probing of lithium based 2-D battery compounds processed by liquid phase exfoliation. Nano Energy, 2016, 30, 18-26.	16.0	8
135	Microelectronics: Stamping of Flexible, Coplanar Microâ€Supercapacitors Using MXene Inks (Adv. Funct.) Tj ETQ	q1_1_0.78 14.9	4314 rgBT /O
136	0D-1D Hybrid Silicon Nanocomposite as Lithium-Ion Batteries Anodes. Nanomaterials, 2020, 10, 515.	4.1	8
137	TEM and EELS characterization of Ni–Fe layered double hydroxide decompositions caused by electron beam irradiation. Npj 2D Materials and Applications, 2021, 5, .	7.9	8
138	Inclusion of 2D Transition Metal Dichalcogenides in Perovskite Inks and Their Influence on Solar Cell Performance. Nanomaterials, 2021, 11, 1706.	4.1	7
139	Charged Domain Wall and Polar Vortex Topologies in a Room-Temperature Magnetoelectric Multiferroic Thin Film. ACS Applied Materials & Interfaces, 2022, 14, 5525-5536.	8.0	7
140	Efficient dispersion and exfoliation of single-walled nanotubes in 3-aminopropyltriethoxysilane and its derivatives. Nanotechnology, 2008, 19, 485702.	2.6	6
141	Bonding States in Molecular-Scale MoSI Nanowireâ^'Gold Nanoparticle Networks. Journal of Physical Chemistry Letters, 2010, 1, 393-397.	4.6	6
142	Hollow Superparamagnetic Microballoons from Lifelike, Self-Directed Pickering Emulsions Based on Patchy Nanoparticles. ACS Nano, 2016, 10, 10347-10356.	14.6	6
143	Silanization of Silica Nanoparticles and Their Processing as Nanostructured Microâ€Raspberry Powders—A Route to Control the Mechanical Properties of Isoprene Rubber Composites. Polymer Composites, 2019, 40, E732.	4.6	6
144	2D nanosheets from fool's gold by LPE: High performance lithium-ion battery anodes made from stone. FlatChem, 2021, 30, 100295.	5.6	6

#	Article	IF	CITATIONS
145	The potential of MXene materials as a component in the catalyst layer for the Oxygen Evolution Reaction. Current Opinion in Electrochemistry, 2022, 34, 101021.	4.8	5
146	Sonochemical edge functionalisation of molybdenum disulfide. Nanoscale, 2019, 11, 15550-15560.	5.6	4
147	Processing and characterisation of Mo ₆ S ₂ I ₈ nanowires. Physical Chemistry Chemical Physics, 2010, 12, 433-441.	2.8	3
148	Synthesis of layered platelets by self-assembly of rhenium-based clusters directed by long-chain amines. Npj 2D Materials and Applications, 2017, 1, .	7.9	3
149	Colloidal Core–Satellite Supraparticles via Preprogramed Burst of Nanostructured Microâ€Raspberry Particles. Particle and Particle Systems Characterization, 2018, 35, 1800096.	2.3	3
150	Growth and analysis of the tetragonal (ST12) germanium nanowires. Nanoscale, 2022, 14, 2030-2040.	5.6	3
151	Mo6S4.5I4.5Nanowires: Structure Studies by HRTEM and Aberration Corrected STEM. Journal of Physics: Conference Series, 2006, 26, 260-263.	0.4	2
152	Study Using Low-loss EELS to Compare Properties of TMDs Produced by Mechanical and Liquid Phase Exfoliation. Microscopy and Microanalysis, 2015, 21, 1475-1476.	0.4	2
153	Laser-powder bed fusion in-process dispersion of reinforcing ceramic nanoparticles onto powder beds via colloid nebulisation. Materials Chemistry and Physics, 2022, 287, 126245.	4.0	2
154	In-situ TEM Analyses over FIB Lamellae - Investigating High Temperature Conversion of Solution Processed Mo-precursor to MoS ₂ Semiconductor Films Microscopy and Microanalysis, 2017, 23, 258-259.	0.4	1
155	A facile route to self-assembled Hg//MoSI nanowire networks. New Journal of Chemistry, 2010, 34, 2241.	2.8	Ο
156	Electronic structure of purified Mo6S(9â^'x)Ix nanowires studied by X-ray spectroscopy. Journal of Electron Spectroscopy and Related Phenomena, 2016, 207, 29-33.	1.7	0
157	Synthesis and Advanced Characterisation of Layered Platelets by Self-assembly of Long-chain Amines. Microscopy and Microanalysis, 2018, 24, 1566-1567.	0.4	Ο
158	Characterizing the Calcination Behaviors of Ni-Fe Layered Double Hydroxide Materials via In-situ Transmission Electron Microscopy. Microscopy and Microanalysis, 2018, 24, 1878-1879.	0.4	0
159	Characterisation and Defect Analysis of 2D Layered Ternary Chalcogenides. Microscopy and Microanalysis, 2021, 27, 642-643.	0.4	0
160	Understanding Degradation Processes in MXene Anodes by In-situ Liquid Cell STEM. Microscopy and Microanalysis, 2021, 27, 1976-1977.	0.4	0